The Quest of Building a Precision TPC Field Cage

Ties Behnke[1], Ralf Diener[1], Oliver Schäfer[1]

[1]Deutsches Elektronen-Synchrotron DESY, Notkestraße 85, 22607 Hamburg, Germany

Abstract. For ILD, one of the detector concepts for the proposed International Linear Collider, a time projection chamber (TPC) is foreseen as the central tracking detector. The R&D effort within the LCTPC collaboration has been centred around a common infrastructure setup operated at the DESY II Test Beam Facility. This setup includes a large field cage as test bed for the different readout technologies to be studied under comparable conditions. A second iteration of this field cage has recently been constructed to improve on the shortcomings noticed with its predecessor. The construction was repeatedly delayed and interrupted due to the COVID-19 pandemic but these delays yielded insights that may not otherwise have been observed during an ordinary course of operations. Methods and findings from the build process are reported.

1 Introduction

This project is part of the design effort for the International Large Detector (ILD) at the future International Linear Collider experiment (ILC) [1]. The FLC-TPC group at DESY Hamburg is part of the LCTPC collaboration [2], which is driving the efforts of developing a TPC for the ILD. Different readout and amplification technologies based on Micro-Pattern Gaseous Detectors (MPGD) are currently studied within the collaboration. For this purpose, a field cage of 75 cm diameter and 57 cm maximum drift length was constructed in 2007 [3]. In order to reach the TPC performance goals for ILD, it combines a low material budget, high voltage stability and high mechanical precision. It features an endplate with mounting space for seven readout modules in three rows (Fig. 1).

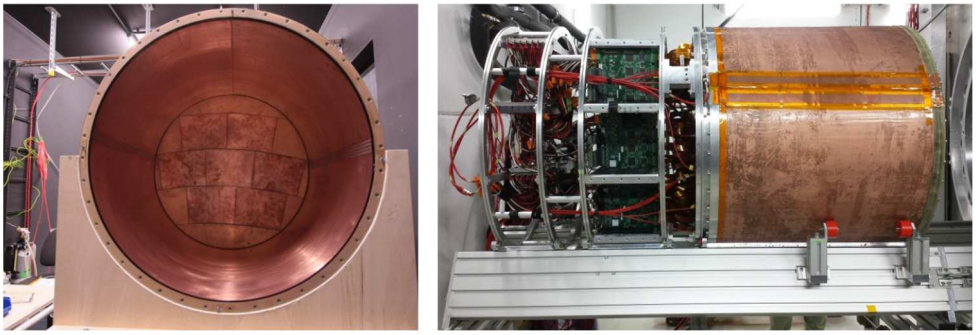

Fig. 1. Large Prototype TPC field cage, first version. **a)** Open. **b)** During a beam test.

In spite of a very successful row of over 30 test beam campaigns by the collaboration with this field cage infrastructure since 2008, it had some known shortcomings. These had been planned to be remedied in a second iteration ever since. Taking up on previous studies for this, a dedicated effort to construct a second field cage was started in October 2019.

2 Design Considerations

The first field cage was produced by an external company. This allowed only limited insight and control of the production process. The resulting field cage was skewed by about factor 10 too much, such that the targeted field homogeneity could not be reached with it, but it was sufficient for many studies of the MPGD readout systems. Besides, detailed control of the material composition was not possible in this mode of fabrication.

For improvement on these issues, it was decided to build the second field cage in-house. This would allow to control the material budget in detail and carefully address the challenging geometrical requirements for the composite material design. Compared to the formerly used simple, shrinkable tube mandrel (Fig. 2a), now a reproducibly precise, collapsible, segmented mandrel with alignment stops was used (Fig. 2b). Assembly strategies, different wall structures, material combinations, and electrical and mechanical properties of these were investigated in numerous pre-tests.

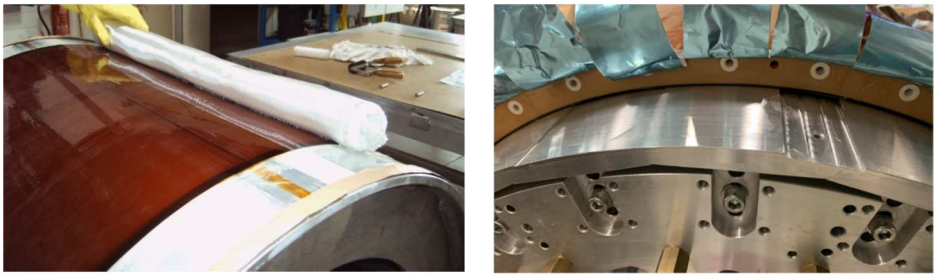

Fig. 2. a) Old mandrel during lamination. **b)** New mandrel in collapsed state.

Also, the implementation of the equipotential rings of the field cage saw some changes. At the time of production of the first field cage there was no production site for a double-sided flexible printed circuit board of the required size (61 cm × 226 cm), thus it was split in two narrow strips that were joined lengthwise later on. Meanwhile it had become possible to produce a full width foil at CERN. The design of the circuit boards was changed as well in favour of a simpler design (Fig. 3b) that requires only half the number of precision resistors. Field distortions reach 7 mm from the wall into the chamber volume, compared to 5 mm with the original field strip design (Fig. 3a).

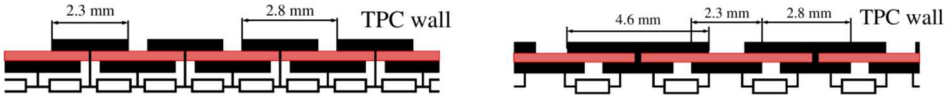

Fig. 3. a) Original strip layout. **b)** Simplified strip layout.

Another change was introduced for the outer shield foil. The previous 50 µm polyimide foil with 10 µm copper cladding was replaced with a 25 µm PET foil with 12 µm aluminium cladding. This yielded a small improvement in material budget by 0.06 %X_0. The foil was also left wider than the field cage length and the excess was cut into strips that serve to establish a low-impedance ground connection between the end plates by clamping. Formerly, a single, narrow copper band was used for that purpose in a mechanically exposed place, crossing the rotational support groove of the TPC.

3 High Precision Resistors

With the new design of the field strip foil came an unexpected challenge. In the first field cage 1 MΩ resistors were used. Those could be measured and sorted with sufficient precision using the 8.5-digit multimeter Agilent 3458A. For the new design 1.5 MΩ resistors were chosen. However, these are just outside of the measurement range of sufficient precision of that device, further complicated by unstable readings of the last digits in that range, in spite of filtering. The absolute resistance of the resistors is largely uncritical for the application. All resistors must be within 50 ppm of the common mean value. Thus, the sorting strategy was changed to a comparison setup based on a Wheatstone bridge.

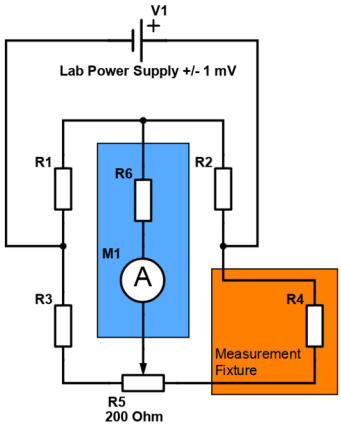

Fig. 4. Wheatstone Bridge.

The bridge (Fig. 4) was composed from three resistors R1 to R3 of the batch of resistors with 500 ppm tolerance to be sorted, and a low resistance potentiometer R5 to equalize the bridge with a fourth, arbitrarily picked reference resistor from the batch. A Keithley Source-Meter 2410 was used as power supply V1 and a freshly calibrated Keithley Electrometer 6514 to measure the bridge current M1. This proved to be a very stable setup, capable of measuring deviations of 7 ppm. For an efficient sorting process, the bridge current was measured and the difference of resistance compared to the reference resistor from the batch was calculated from it.

The method is very precise, because the resistor batch is already pre-sorted and thus there are only small deviations that will cause small bridge currents. These can be measured with sufficiently sensitive devices (order of nanoampere, in this case) without the need for a big measurement range or multimeters of utmost precision. In addition, the supply voltage and ambient temperature were logged, and the bridge re-zeroed with the reference resistor to recognize and avoid long-term systematic shifts.

The setup was first used with a measurement fixture to sort the SMD resistors straight from the tape reel (Fig. 5a). Later a modified fixture was built to measure the resistors again in their equipped state on the field strip foil (Fig. 5b) to assess possible effects from the soldering process. In both setups there was the problem of a settling time of a few ten seconds before each measurement. The readout of the setup was thus automated. The measured values were logged graphically at first, to evaluate the settling process visually. Soon this solution was extended with an online analysis based on the interquartile range as a statistical criterion to assess the settling process. The standard deviation versus 10 % of the bin width was used to ensure a sufficient number of measurements for reliable sorting into 50 Ω bins.

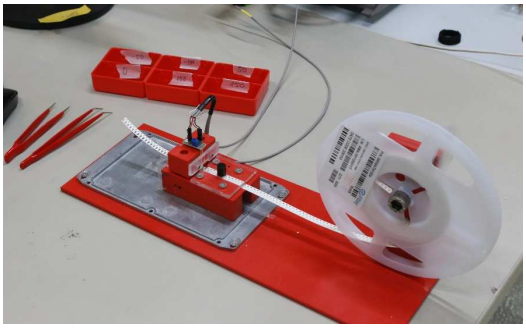

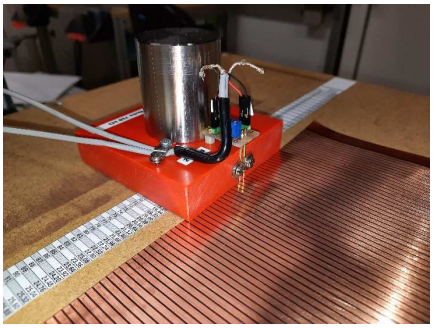

Fig. 5. a) Resistor sorting fixture. **b)** Foil measurement fixture.

4 Field Strip Foil

4.1 Preparation

The new field strip foil was produced at CERN from a 50 µm polyimide base material with 17 µm copper cladding on both sides. Compared to the previously used 35 µm copper cladding this improved the material budget by about 0.25 %X_0. Of four foils, which arrived in June 2020, three had obvious electric defects, like short-circuits between strips. With these especially the precision cutting of the foil was investigated. Apart from precise alignment along the edges on the mandrel, also the resulting gap between the foil ends should be kept in the order of 100 µm.

4.2 Low Voltage Testing and Repair

In November 2020 the one good foil was equipped with the sorted batch of precision resistors and tested again. At that point one place in the resistor chain showed a significant deviation of 100 kΩ. The expected resistance between strips is 750 kΩ, due to two resistor chains being connected to the strips in parallel. As replacing the resistors did not yield any improvement, another parasitic high impedance connection was assumed. Impurities on the cut edges could be excluded. likewise, the field strip foil was lying on an insulating plastic foil. A comparison of signal runtime between the faulty strips and two strips without problem (Time Domain Reflectometry) finally allowed a rough localization of the fault (Fig. 6a). Upon closer inspection with a microscope a slight bulge in the copper cladding was found (Fig. 6b), which covered a tiny hole of about 0.5 mm diameter (Fig. 6c).

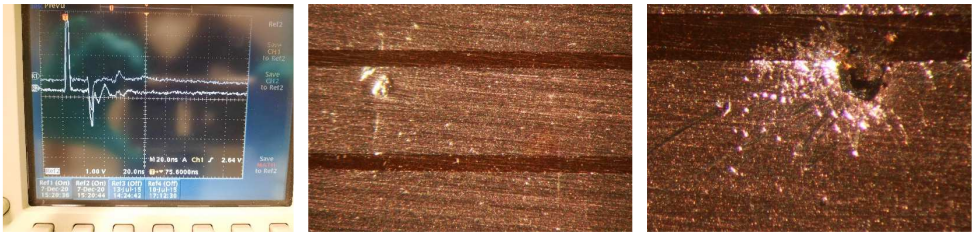

Fig. 6. a) TDR signals of a good and the faulty strip. **b)** Fault location. **c)** Opened hole (gap: 0.5 mm).

As the resistance measurement was still connected at about 20 V, minute sparking could be observed inside the hole through the microscope. Taking video footage of these sparks [4] the growth mechanism of the hole could be documented (Fig. 7c). It was an interplay of sparks that erode the copper surface (Fig. 7a) and char the polyimide foil, and the charred polyimide becoming conductive, heating up by the current to a red glow and eventually burning (Fig. 7b). Even small wisps of smoke could be observed through the microscope.

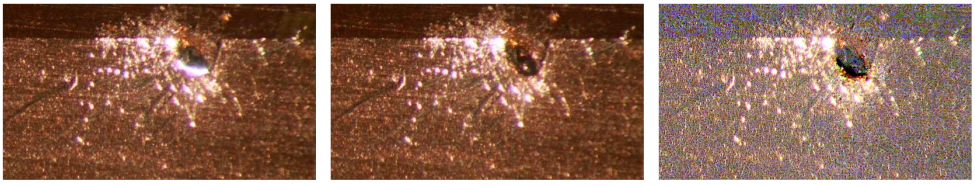

Fig. 7. a) Sparking along copper edge. **b)** Glowing carbonized polyimide. **c)** Calculated before-after comparison, black areas mark evaporated parts.

The damaged spot was carefully cut out, filled with epoxy resin and covered with two polyimide patches of 3 mm diameter to provide extra insulation path. The field strip pattern was then painted onto the patches with silver paint. Testing of the repaired spot was planned after curing of the resin. However, due to COVID-19 measures further work could only resume in September 2021.

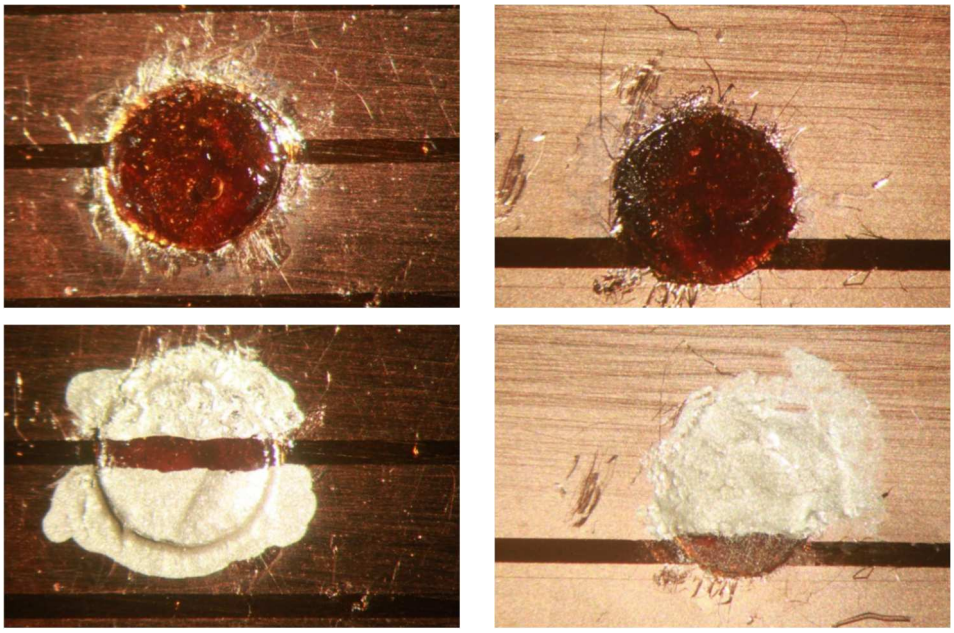

Fig. 8. Repair on field strip side (left) and mirror strip side (right).

The entire foil was measured again with the specially constructed measurement head. Proceeding strip-wise across the foil, the measurements showed a systematic shift of a few 100 Ω and still a deviation of 2 kΩ for the repaired strips. Besides, a notable charge-up behaviour was present in most measurements. To mitigate this, it was tried to perform the measurements on an ESD protection mat, however, its resistance was too low and biased the measurements. Measuring directly on the wooden surface of the table removed the charge-up behaviour and the majority of the resistors were within a 50 Ω band, similar to the bins of the sorted resistors. Also, the deviation of the repaired strip had shrunk to 1 kΩ.

This trend continued until subsequent measurements in January 2022, performed on a different spot on the table surface and with possible noise sources, like metallic sources and the temperature sensor removed from the immediate measurement location. Only the repaired strip was then still outside the 50 Ω band by merely 40 Ω (Fig. 9). When the measurement was repeated a week later, to check for a possible exchange, even this difference had vanished and all resistors were now within the targeted 50 ppm tolerance band of 75 Ω.

The current assumption for this long-term behaviour is that the complete curing of the epoxy resin actually took a year. Besides, air bubbles where trapped under the polyimide patches (Fig. 8.), which likely contained some moisture.

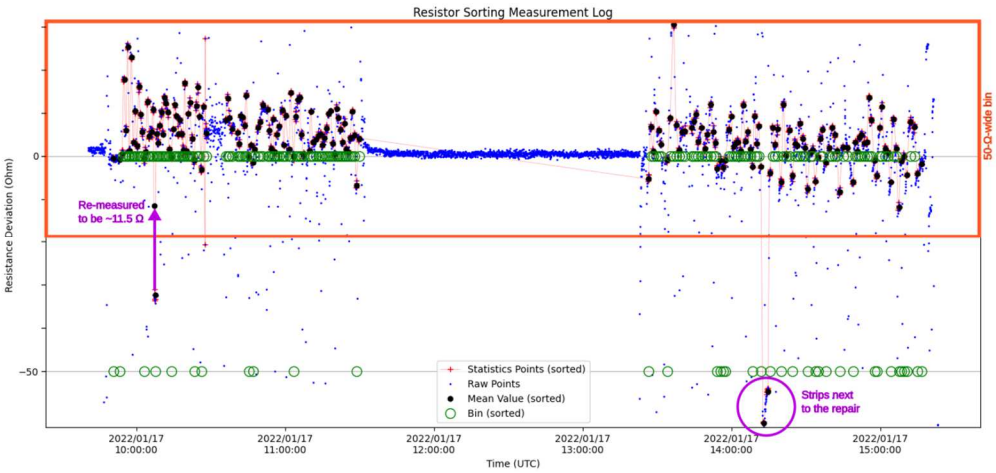

Fig. 9. Example of a log of field strip resistance measurements with one last outlier.

4.3 High Voltage Tests

After considerable safety precautions an open high voltage test of the field strip foil were performed end of April 2022. This consisted of a quick test with 30 kV over a few minutes and a test with 25 kV over 24 hours. Both tests were passed without any problems.

Fig. 10. Open high voltage test setup of field strip foil.

5 Field Cage Construction

With the successfully completed high voltage tests, the lamination of the field cage could finally start in June 2022. Initially, the field strip foil was carefully aligned on the precision mandrel (Fig. 11a). After gluing the flange rings in place, using the end stops, subsequently layers of glass fibre and honeycomb were laminated. For each step the amount of glue was carefully recorded to track the material budget. Before the outer layers of the field cage could be laminated an excess of honeycomb material needed to be removed by routing (Fig. 11b). However, the next layers bonded considerably worse than in previous tests. Due to the global delivery crisis at that time, new material only arrived in spring 2023 and the field cage could be completed in April 2023 (Fig. 11c).

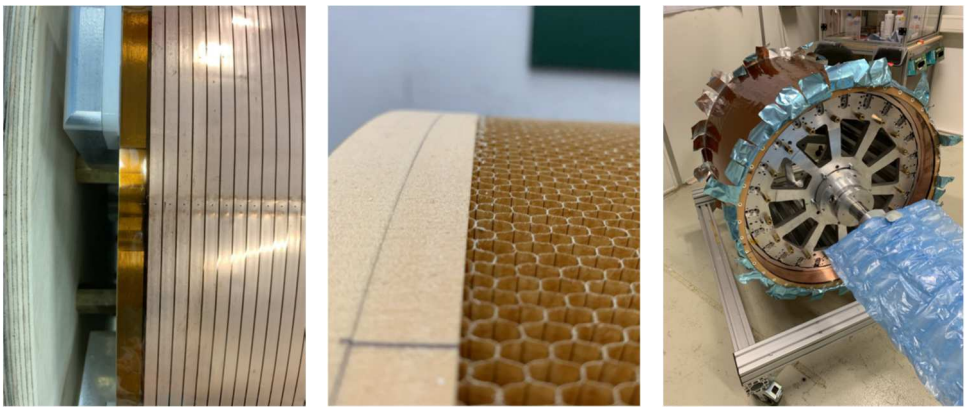

Fig. 11. a) Alignment of field strip foil. **b)** Routed flange honeycomb transition. **c)** Completed field cage being removed from the mandrel.

6 Geometric Survey

In June 2024 a geometrical survey of the field cage was undertaken. However, the results are not directly comparable with those of the first field cage, as the measurement equipment had been changed in the 15 years between the two builds. Both field cages were surveyed with a measuring-arm. While the old arm had sufficient reach and precision for the entire field cage, this was not the case for the new equipment. One arm had sufficient reach, but was less precise (order of 100 µm) than the one used on the first field cage. Another was more precise, but did not have enough reach to measure both sides. Furthermore, it was difficult to locate features like the field strip edge reliably with the probe.

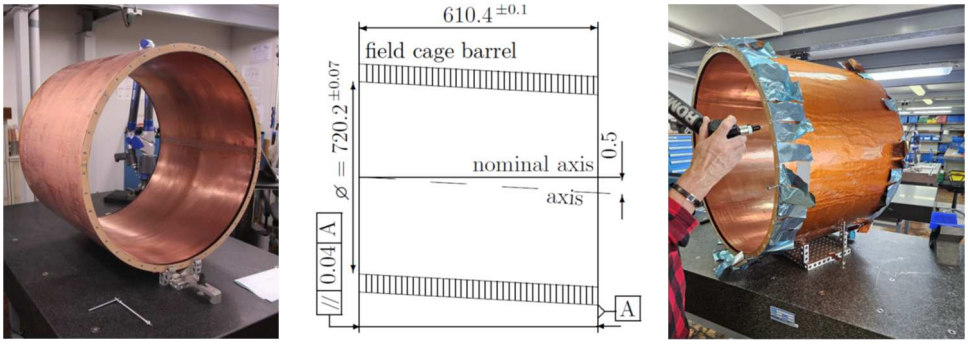

Fig. 12 a) Survey of first field cage. **b)** Survey results of first field cage. **c)** Survey of new field cage.

Nonetheless, the preliminary results with the long-reach arm suggest that the skew of the field cage could be significantly improved with respect to the first field cage (about 70 µm). However, other aspects of the build seem to be worse. One flange is tilted and out of parallel to the other by about 400 µm. The alignment of the field strips with respect to the flanges and at the seam of the foil is off by about 200 µm. As great care was taken for the initial alignment of the field strip foil on the mandrel, the cause for these deviations are likely shifts induced by the tool movements during the lamination process.

A more precise survey is needed to quantify these preliminary observations reliably and assess possible countermeasures. For example, other components of the TPC, like the cathode, can be adjusted for tilt. Thus, it could compensate for a tilted mounting flange.

Summary and Acknowledgement

A new, improved field cage for the Large Prototype TPC was foreseen to be ready in spring 2020. COVID-19 and parallel priority workload of everyone involved caused extreme delays. Thanks to the continued steady effort of the former TPC group at DESY and especially our technical staff Ole Bach, Bernd Beyer, Andreas Busch, Volker Prahl, and the support of the central electronics group and quality control group at DESY, the second field cage could finally be completed in April 2023. Inhouse experience for such a construction was gained and methods for resistor sorting, fault detection and repair in flexible circuit boards were developed. The propagation and growth of electrical insulation faults in copper-clad polyimide foil could be filmed. This might give new insights for similar applications of such foils in MPGD.

References

1. T. Behnke, J. E. Brau et al., eds. The International Linear Collider. Technical Design Report. Vol. 4: Detectors. Linear Collider Collaboration, 2013.
   arXiv: https://arxiv.org/abs/1306.6329
   url: https://www.linearcollider.org/
2. Homepage of the LCTPC collaboration.
   url: https://www.lctpc.org/
3. T. Behnke, K. Dehmelt et al., A lightweight field cage for a large TPC prototype for the ILC. JINST **5.10**, p. 10011 (2010).
   doi: https://doi.org/10.1088/1748-0221/5/10/P10011
4. O. Schäfer, T. Behnke, R. Diener, Spark Damage Mechanism of Copper-Clad Polyimide Foil, Video.
   doi: https://doi.org/10.3204/PUBDB-2024-06696